# *In Situ* Compatibilization of Low-Density Polyethylene and Polydimethylsiloxane Rubber Blends Using Ethylene–Methyl Acrylate Copolymer as a Chemical Compatibilizer

R. N. SANTRA,[1] B. K. SAMANTARAY,[2] A. K. BHOWMICK,[1] and G. B. NANDO[1,*]

[1]Rubber Technology Centre and [2]Department of Physics, Indian Institute of Technology, Kharagpur-721 302, India

**SYNOPSIS**

The effect of the ethylene–methylacrylate copolymer as a chemical compatibilizer in the 50 : 50 blend of low-density polyethylene (LDPE) and polydimethylsiloxane rubber (PDMS) has been studied in detail. Ethylene–methylacrylate (EMA) reacted with PDMS rubber during melt-mixing at 180°C to form EMA-grafted PDMS rubber (EMA-*g*-PDMS) *in situ*, which acted as a compatibilizer in the LDPE–PDMS rubber blend. An optimum proportion of the compatibilizer (EMA) was found to be 6 wt % based on results of dynamic mechanical analysis, adhesion studies, and phase morphology. Lap shear adhesion between the phases increased significantly on incorporation of 6 wt % of EMA. Dynamic mechanical analysis showed a single glass transition ($T_g$) peak at −119°C. This was further supported by X-ray diffraction studies, which exhibited a remarkable increase in the degree of crystallinity and phase morphology and showed a drastic reduction in the size of the dispersed phase at the optimum concentration of EMA. 

## INTRODUCTION

Blending of thermoplastics and elastomers have become an increasingly important area of research activity in recent years. Voluminous work[1,2] has been carried out in this area to understand the mechanical, thermal, and processing behavior of these blends that could be correlated with changes in the structure and phase morphology of the blends. Of the many thermoplastics and elastomer blends studied so far, only a few have become technologically feasible and commercially viable because of their enhanced mechanical properties, ease of processing, higher thermal stability, and comparatively lower cost. From this emanated the concept of polymer–polymer compatibility. Compatibility arises from thermodynamic interaction between the blend constituents, which is a function of their physical and chemical structures.[3] Most of the blends in a multicomponent polymer system are found to be incompatible for a variety of reasons such as the absence of any specific interaction between their blend constituents, dissimilarity in their structures, and broad differences in their viscosities, surface energy, or activation energy of flow and polarity. Nevertheless, such blends are commercially important because they combine the unique properties of both the constituents in the blend for specific applications. However, the phenomenon of compatibility can be induced into an immiscible polymer–polymer pair in a binary system by introducing a third component that will either interact with both the phases chemically or will have specific interaction with one phase and physical interaction with the other. It may be emphasized here that the function of the third component is to reduce the interfacial tension between the two phases, increase the surface area of the dispersed phase, promote adhesion between the phase components, and stabilize the dispersed phase morphology. It has functional similarity to that of an emulsifying agent in an immiscible binary liquid system and therefore is known as an "interfacial agent" or, popularly, as a "compatibilizer" in the polymer industry. Xanthos[4] gave a detailed account of various interfacial agents used as compatibilizers in the multiphase polymer systems. The

* To whom correspondence should be addressed.

Journal of Applied Polymer Science, Vol. 49, 1145–1158 (1993)
 CCC 0021-8995/93/071145-14

most common practice is the introduction of a compatibilizer capable of specific interaction or chemical reaction with at least one of the blend constituents.[5]

Depending on the processing conditions, in an immiscible multiphase polymer melt, the phase present in the larger volume represents the continuous phase and the minor phase is the dispersed or discontinuous phase. Where both phases are present in equal proportions, differing widely in their viscosities, then the phase having the lower viscosity becomes the continuous phase. This has been observed by the authors[6] earlier in a 50 : 50 blend of low-density polyethylene and polydimethylsiloxane rubber melt mixed at 120 and 180°C, respectively, by studying the phase morphology. This immiscibility is primarily due to structural dissimilarity, lack of specific interaction between the blend constituents, and a wider difference in their surface energies (13 J/m). This causes slippage between the phases during processing and molding, leading to poor physicomechanical properties and an unstable phase morphology. However, blending the constituents with a functionalized copolymer having specific interactions and/or chemical reactions with the blend constituents should result in improvement of physicomechanical properties and stability of the phase morphology.

Willis and Favis[7] studied the processing and phase morphology relationship of compatibilized polyolefin–polyamide blends with the help of an ionomer compatibilizer. They found that there is an abrupt increase in dispersion and interfacial adhesion and a decrease in the particle size of the dispersed nylon phase. This was reported to be due to specific interaction between nylon and the ionomer at the interface in a blend of polyethylene and nylon. Similarly, Molnar and Eisenberg's[8] succeeded in compatibilizing nylon and polystyrene through functionalization of polystyrene.

Recently, Song and Baker[9] reported that *in situ* compatibilization of polystyrene and polyethylene blends is possible with the help of aminomethacrylate-grafted polyethylene. They prepared blends of styrene maleic anhydride with polyethylene as well as blends of polyethylene melt-grafted with secondary or tertiary aminomethacrylates. The latter blends were found to give improved mechanical properties and finer morphology as compared to the former ones, which was explained as due to chemical interaction of the acidic anhydride and basic amino groups.

The objective of the present investigation was to compatibilize a blend of low-density polyethylene (LDPE) and polydimethylsiloxane (PDMS) rubber having no affinity to each other and dissimilarity in structure, with the help of a third component that will act as an emulsifier at the interface by modifying one of the component phases at the interface. A copolymer of ethylene–methylacrylate (EMA) containing 21% of methylacrylate was chosen as the third component in this system.

In the present investigation, for convenience and clarity, a blend of LDPE and PDMS rubber in the proportion of 50 : 50 was chosen. EMA copolymer was added as the compatibilizer in a proportion varying from 1 to 10 wt % to study its action on the blend properties. This paper deals with the study of the following parameters:

(i) Mechanism of action of the EMA copolymer as a chemical compatibilizer in the blend of LDPE and PDMS rubber.
(ii) Effect of the EMA copolymer on the adhesion between the component phases.
(iii) Effect of the EMA copolymer on impact strength and phase morphology of the blend.
(iv) Effect of the EMA copolymer on the rubber–glass transition temperature ($T_g$) of the blend.
(v) Effect of the EMA copolymer on the microstructure of the blend.

## EXPERIMENTAL

### Materials

Low-density polyethylene (LDPE) (Indothene 20XL020) having a density of 919 kg $m^{-3}$, MFI of 2.0 g/10 min, and melting point of 112°C was supplied by Indian Petrochemicals Corp., Badodara, India. Polydimethylsiloxane rubber (silastic WC-50) having a density of 1150 kg $m^{-3}$ and brittle point of −39°C was supplied by NICCO Corp., Athapur, Calcutta, India. Ethylene–methylacrylate (EMA) copolymer resin (OPTEMA TC-120) containing 21% methylacrylate and with a melt index of 6.0 dg/min, density of 940 kg $m^{-3}$, and melting point of 81°C was supplied by Exxon Chemicals Eastern Inc., Bombay, India.

### Preparation of the Blend

Polyethylene, PDMS rubber, and EMA were melt-mixed in a Brabender Plasticorder Model PLE 330 with cam-type rotors at 180°C and 100 rpm rotor sped for 5 min. The proportion of LDPE and PDMS rubber were kept constant at 50 : 50 and EMA content was varied from 1 to 10 phr. The molten mass was sheeted out immediately on a two-roll mixing mill and subsequently compression-molded in a

Labo press at 180°C for 5 min at a pressure of 10 MPa, cooling the sheets under pressure by passing cold water through the platens of the Labo press.

### Tensile Impact Strength Test

The molded sheets were stripped out of the cool mold and dumbbell specimens were punched out with a hollow cutting die (Die-C). Tensile impact strength of the blends was performed by a Ceast impact testing machine (Model 6564/000) fixed with a load cell of 7.5 N at room temperature using the dumbbell test specimens. The impact energy was recorded and the impact strength was expressed in J/m.

### Preparation of Samples for Lap Shear Adhesion Test

#### *Type I Assembly*

Various doses of EMA copolymer was melt-mixed with LDPE at 120°C and at 100 rpm rotor speed in the Brabender plasticorder and compression-molded to tensile sheets in the Labo press at 120°C under a pressure of 10 MPa, taking sufficient care to protect one side of the sheet with a cellophane paper/aluminum foil. After cooling to room temperature in the Labo press, strips of 75 × 25 mm were cut from the sheets and cellophane paper was gently stripped off. The strips were laid one over the other, sandwiching a thin layer of PDMS rubber (2 mm) so that a 25 × 25 mm area of the strips was overlapped toward the ends, as shown in Figure 1. The assembly was then hot-pressed in a specially designed mold in the Labo press at 180°C for 5 min under a pressure of 0.2 MPa, to allow the reaction between EMA and PDMS rubber to take place at the interface. This assembly was termed as a lap shear test specimen and designated as specimen type I.

#### *Type II Assembly*

In the second stage, EMA copolymer in various doses was melt-mixed with PDMS rubber in the Brabender plasticorder under similar conditions and subsequently molded to sheets 2 mm thick, as described above. Similarly, neat LDPE was molten in the plasticorder at 120°C and sheeted out in the Labo press to 2 mm thick. Strips of LDPE of 75 × 25 mm were cut out from the sheet and the test assembly was made by sandwiching the EMA–PDMS rubber blend between the two LDPE strips to form an overlapped area of 25 × 25 mm toward the ends. Subsequently, the assembly was hot-pressed in the Labo press at 180°C for 5 min for the reaction to occur and the samples were designated as specimen type II.

Finally, the lap shear test was performed in a Zwick UTM (Model 1145) at room temperature at a crosshead speed of 50 mm/min and the results were expressed in $N/cm^2$.

### IR Studies

Blends of LDPE and PDMS rubber, and that containing 6 wt % of EMA, were prepared by the melt-mixing technique at 180°C. Thin films of approximately 0.1 mm thick of the pure components and the blends were compression-molded in the Labo press at the same temperature. Infrared spectroscopic studies of the samples were performed with a Perkin-Elmer IR spectrophotometer (Model 843) in the wavelength range of 200–4000 $cm^{-1}$.

### Dynamic Mechanical Analysis

Dynamic mechanical analysis of the LDPE–PDMS rubber blends containing various doses of EMA were performed in a Rheovibron Model DDV III EP at a frequency of 3.5 Hz and in the temperature range varying from −150 to +150°C. The size of the samples used was 7 × 0.5 × 0.4 cm.

### SEM Studies

Phase morphology of the blends was studied by examining the etched surfaces of the blends under a scanning electron microscope model Cam Scan Series II. Pellets were punched out of the molded sheets and etched in toluene for 48 h at room temperature to drive out unmodified PDMS rubber. The solvent-extracted samples were dried in a vacuum oven at 70°C for 12 h and cooled to room temperature in a desiccator. Subsequently, the etched surfaces were

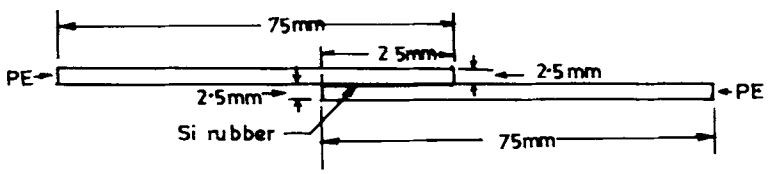


**Figure 1** Lap shear adhesion test sample.

sputter-coated with gold for facilitating scanning under the SEM at a 0° tilt angle.

## Wide-angle X-ray Scattering Studies (WAXS)

The blends containing various proportions of EMA were subjected to wide-angle X-ray diffraction studies using monochromatized CuK$\alpha$ radiation using a nickel filter and a diffractometer (Philips PW 1729 X-ray generator).

The diffraction was recorded in the angular range from 7° $2\theta$ to 50° $2\theta$ at a scanning speed of 3° per min. The degree of crystallinity of the neat EMA and that of the blends were calculated from the diffractograms following the method of Herman and Weidinger.[10] The values of crystallite size and the root mean square paracrystalline distortion parameter were calculated for the (1, 1, 0) and (2, 0, 0) directions from the integral breadths of the line profiles.[11] Preferred orientation of the different crystallites with respect to the surface of the blend was evaluated from the ratio of the integrated intensity of reflections. The value of the interchain distance was estimated from the maxima of the X-ray intensities.[12]

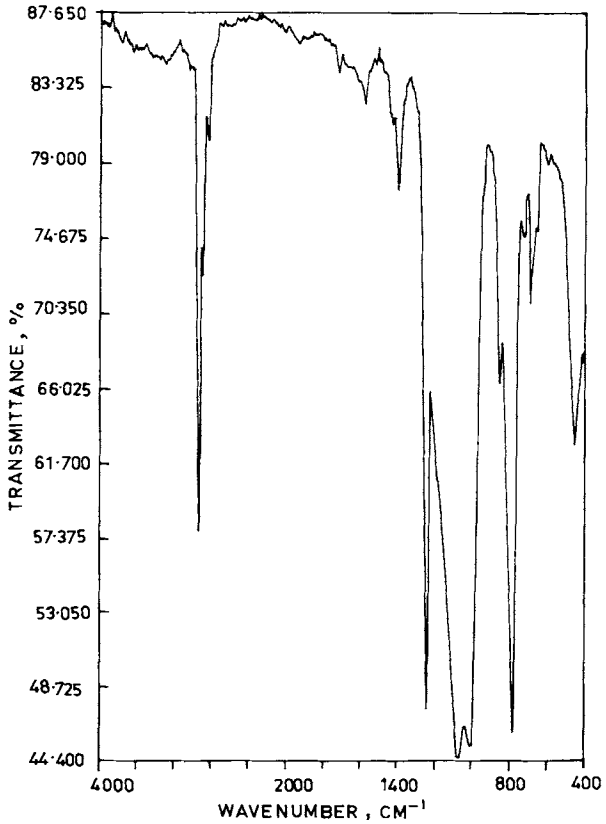


**Figure 2** IR spectrogram of PDMS rubber.

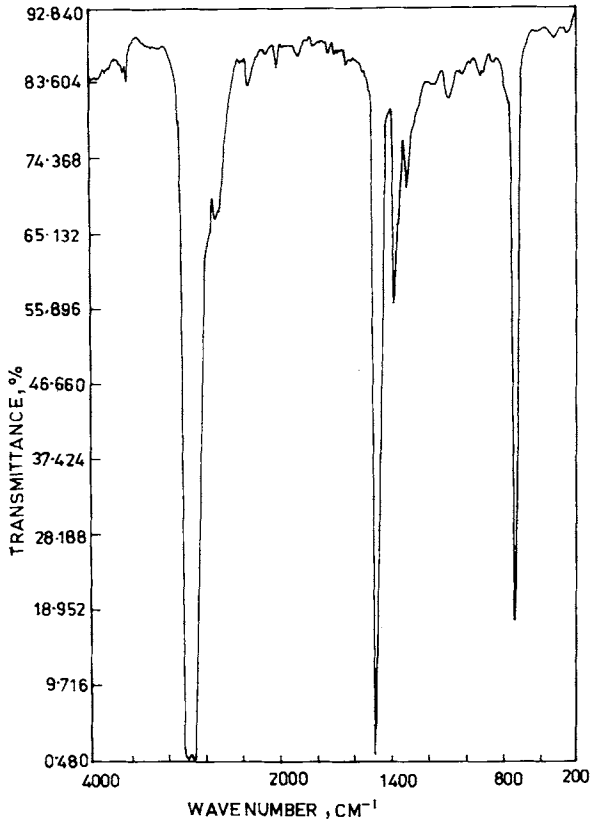


**Figure 3** IR spectrogram of LDPE.

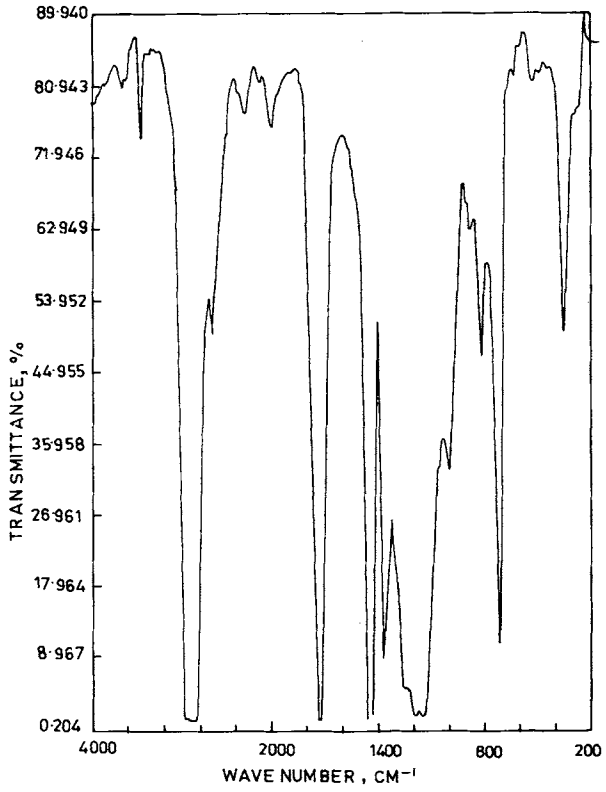


**Figure 4** IR spectrogram of EMA copolymer.

## RESULTS AND DISCUSSION

### Mechanism of Action of EMA Copolymer in the Blend by IR Study

Infrared spectrograms of the individual blend components and the blend containing 6 wt % of EMA are shown in Figures 2–5. The IR spectrum of PDMS rubber (Fig. 2) reveals the presence of vinyl groups attached to the silicone atom as evidenced from the C=C stretching at 1597 $cm^{-1}$ and in-plane vibration of the vinyl $HC=CH_2$ group at 1409 $cm^{-1}$.[13] The IR spectrum of LDPE shows a $-CH_2-$ rocking vibration at 1462 $cm^{-1}$ and methyl branching at 1375 $cm^{-1}$, evidence of minor chain branching of LDPE (Fig. 3). The IR spectrum of the EMA copolymer reveals the presence of ester groups from the strong peak at 1733 $cm^{-1}$ (Fig. 4). But IR spectra of blends of LDPE and PDMS rubber in the proportion of 50 : 50 mixed at 120 and 180°C, respectively, do not exhibit any extra peak except those of LDPE and PDMS shown in Figure 5. This provides ample evidence for the absence of any specific interaction or chemical reaction between the two. However, the IR spectrum of a blend of LDPE and PDMS in the proportion of 50 : 50 containing 6 wt % of EMA shows a reduction in the C=C stretching peak at 1597 $cm^{-1}$, indicating that a part of the vinyl group has been utilized in the reaction with EMA during melt processing. The absorbance ratio, Ar (Ar = A1597/A1462, where A1597 and A1462 are the absorbance at 1597 and 1462 $cm^{-1}$, respectively) as per the ASTM D-3677 method also shows a decrease with respect to the 50 : 50 blend of LDPE–PDMS rubber without EMA. The Ar value for the LDPE–EMA–PDMS rubber terblend was found to be 0.03 and that for LDPE–PDMS was 0.04; thus, a reduction in the absorbance ratio of C=C for the terblend was found to be 25% as reflected in the superimposed IR spectra of LDPE–PDMS and

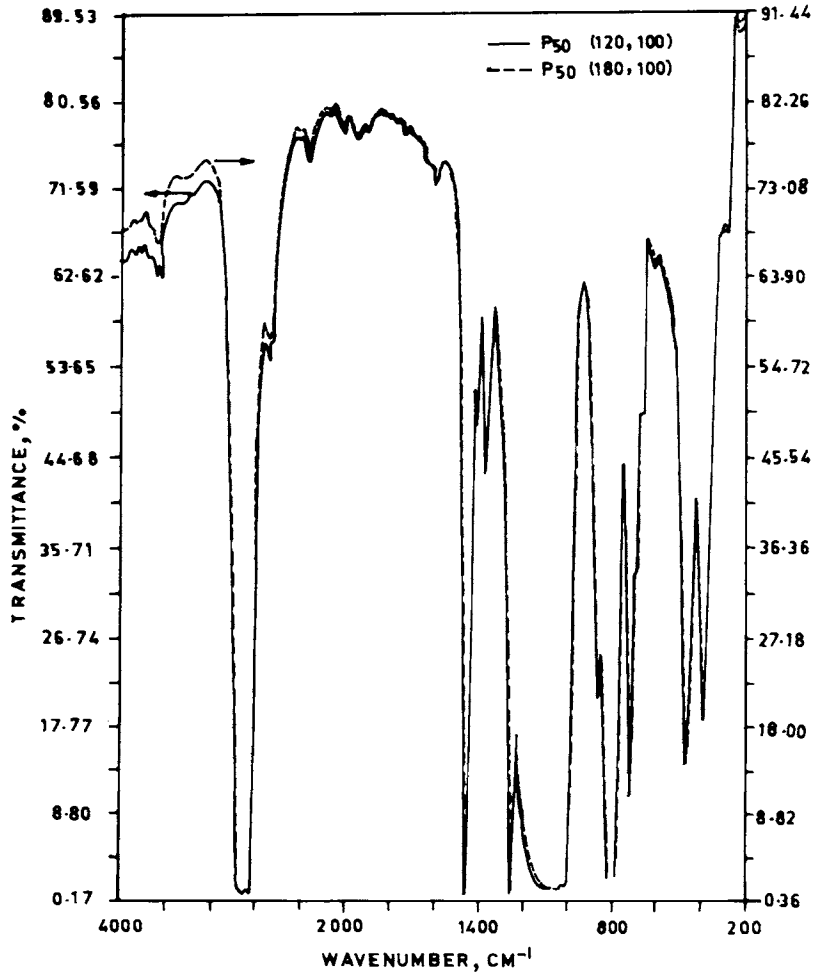


**Figure 5** IR spectrogram of LDPE : PDMS (50 : 50) blend denoted as P50, processed at 120 and 180°C.

LDPE–EMA–PDMS blends (Fig. 6). This strongly supports the view that there is strong interaction via chemical bond formation between the PDMS rubber and EMA copolymer. This phenomenon has been explained below and a plausible mechanism has also been suggested.

### *Step I*

The labile hydrogen atom at each $\alpha$-carbon atom adjacent to the ester group of the EMA breaks homolytically to give a H radical and A radical during melt processing under shear:

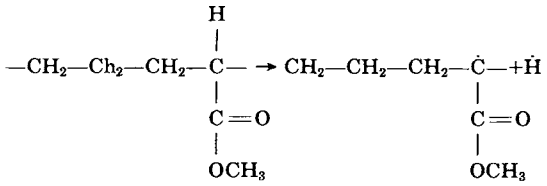

(A)

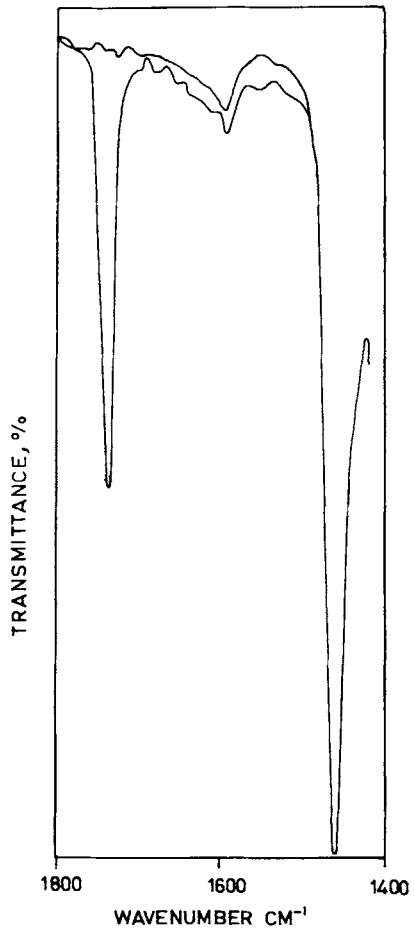


**Figure 6** Superimposed IR spectrogram of LDPE–PDMS rubber blend and LDPE–PDMS rubber blend containing 6 wt % of EMA copolymer.

The Ḣ radical thus generated, being unstable, combines with another Ḣ radical generated at another site, forming $H_{2\uparrow}$ gas in trace amounts, which escapes out.

### *Step II*

The free radical Ȧ thus generated in step I is stable and may attack the vinyl site of the PDMS rubber to give the intermediate Ḃ or Ċ:

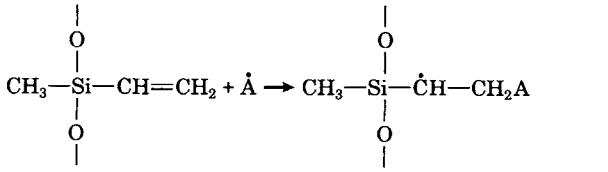

(Ḃ)
or

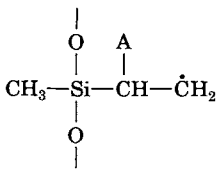

(Ċ)

Of these two, formation of Ḃ is preferable because it encounters less steric hindrance.

### *Step III*

The intermediate B then abstracts a H radical from another EMA molecule and becomes saturated. Consequently, a new Ȧ macroradical is generated and the process continues. This is shown as

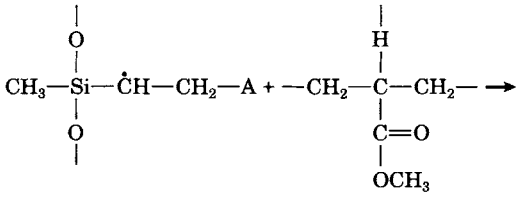

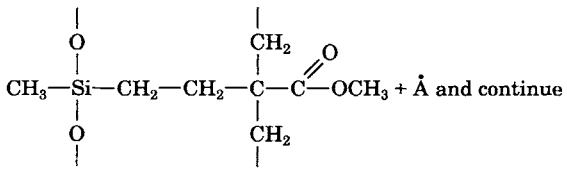

(EMA-*g*-PDMS)

As a result, a carbon–carbon bond is formed between the EMA copolymer and the PDMS rubber through the $-CH_2-CH_2-$ bridge, leading to EMA-grafted PDMS rubber (EMA-*g*-PDMS).

### Effect of the EMA Copolymer on the Lap Shear Adhesion and Phase Morphology of the LDPE–PDMS Rubber Blend

The lap shear adhesion strength of the LDPE and PDMS rubber blends containing EMA in one of the phases separately were carried out and the results are shown in Table I. Because of very weak matrix strength of PDMS rubber, it was not possible to carry out a peel adhesion strength of the blends with PDMS rubber as one of the adherends.

The lap shear adhesion strength of the type I assembly increases gradually from 2.6 to 5.0 N/cm$^2$ as the proportion of EMA copolymer in LDPE increases from 0 to 10 wt %. The increase in lap shear strength is rapid up to 4 wt % of EMA in the polyethylene phase, beyond which the increase is marginal up to 10 wt % of EMA. This is a clear indication of the fact that the optimum concentration of EMA in LDPE should lie between 4 and 10 wt %. This is obviously due to the reaction of EMA with PDMS rubber at the interface forming the EMA-grafted PDMS (EMA-*g*-PDMS) that acts as a compatibilizer, thus reducing the surface tension of polyethylene.

In case of type II specimens where EMA in proportions of 4–10 wt % is added to PDMS rubber separately and then adhesion strength against LDPE substrates is measured, the lap shear adhesion strength is found to be higher as compared to that with type I assembly. Interestingly, there is an abrupt increase in adhesion strength when EMA concentration is increased from 4 to 6 wt %. Beyond 6 wt % of EMA, the increase of strength was marginal. This is obviously due to greater chemical interaction between EMA and PDMS rubber, which enhances the modulus of the PDMS rubber, resulting in increased adhesion strength. Second, since EMA-*g*-PDMS rubber acts as an emulsifier at the interface and reduces the surface energy of polyethylene, the wetting of polyethylene with PDMS rubber also increases, supporting the aforesaid observation. The marginal increase in adhesion strength beyond 6 wt % of EMA in PDMS rubber may be due to the greater interaction between the two phases. This has been further evidenced by the SEM studies of the molded and solvent-etched specimens of LDPE–PDMS rubber blends containing different proportions of EMA, as discussed below:

**Table I Adhesion Strength of the LDPE and PDMS Rubber Blends Containing EMA**

| Sample Code | Adhesion Strength (N/cm$^2$) |
|---|---|
| $PE_0$ | 2.6 |
| $PE_2$ | 3.2 |
| $PE_4$ | 4.1 |
| $PE_6$ | 4.3 |
| $PE_{10}$ | 4.5 |
| $Si_0$ | 2.6 |
| $Si_4$ | 4.2 |
| $Si_6$ | 7.0 |
| $Si_{10}$ | 7.3 |

The subscripts represent the proportion of EMA in each phase.

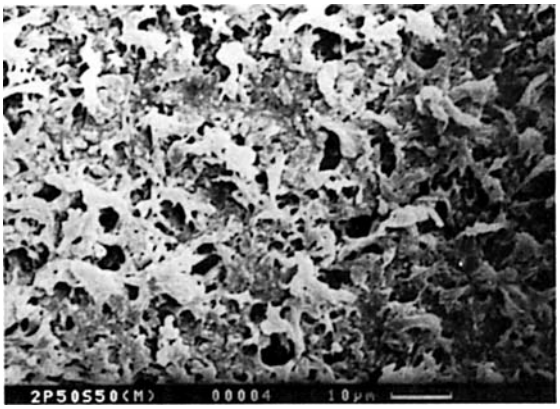


**Figure 7** SEM photomicrograph of polyethylene–PDMS rubber blend (50 : 50) at 1100× (10 μm).

The phase morphology of the LDPE–PDMS rubber blends are shown in Figures 7–9. Figure 7 shows the SEM photomicrograph of a 50 : 50 blend containing no compatibilizer. It shows a loose matix with an irregular domain size and shape of PDMS, giving rise to the appearance of a spongy matrix due to etching out of PDMS rubber. We can expect that polyethylene and PDMS rubber were present in a cocontinuous form in the blend. Incorporation of 6 wt % of EMA reduces the dispersed domain size of

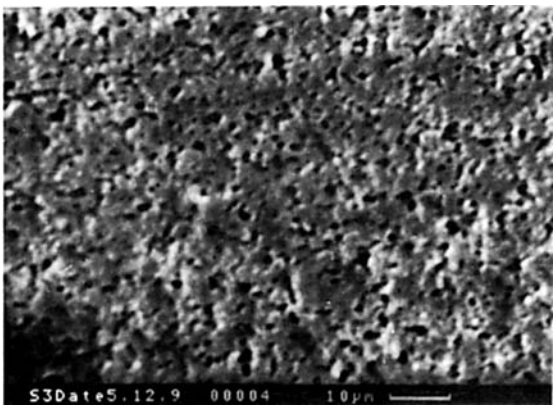


**Figure 8** SEM photomicrograph of polyethylene–PDMS rubber blend containing 6 wt % of EMA copolymer at 1100× (10 μm).

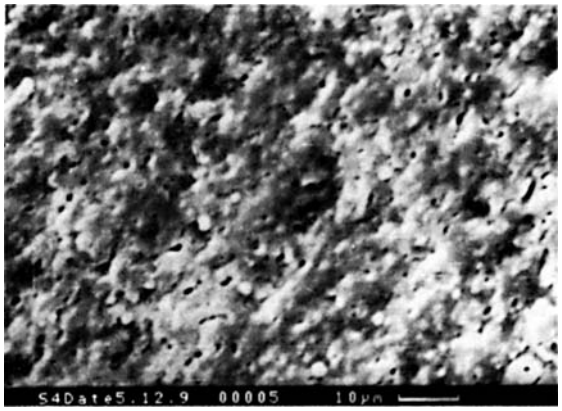


**Figure 9** SEM photomicrograph of polyethylene–PDMS rubber blend containing 10 wt % of EMA copolymer at 1100× (10 μm).

PDMS rubber, as evidenced from the SEM photomicrograph of Figure 8. Here, uniform dispersion as well as distribution of the dispersed phase (PDMS rubber) takes place. Increasing the EMA proportion to 10 wt % reduced the dispersed phase size of PDMS rubber further because of better compatibilization, as shown in Figure 9, but PDMS rubber could not be completely gotten rid of due to excessive reaction with EMA, resulting in the formation of a separate EMA-*g*-PDMS phase in the system. Thus, EMA acts as a chemical compatibilizer by reacting with PDMS rubber, on the one hand, and by cocrystallizating with polyethylene, on the other hand, because of its structural similarity with LDPE. EMA reduces the particle size of the dispersed domain from 3.3 to 1.1 μm when incorporated in a 6 wt % level, which is evidence for an increased surface area of the dispersed phase morphology and an effective compatibilization that is responsible for the increased adhesion strength between the blend components. Thus, 6 wt % of EMA copolymer is considered to be the optimum level for compatibilizing a 50 : 50 blend of LDPE–PDMS rubber. The reduction in particle size of the dispersed phase domain is further proved from impact strength studies of the blends.

## Effect of EMA Copolymer on the Impact Strength of LDPE–PDMS Rubber Blend

The tensile impact strength of LDPE–PDMS rubber blends containing EMA in proportions varying from 1 to 10 wt % is given in Table II. The impact strength of the blend improves significantly with EMA incorporation. The impact strength increase was from 765 to 1760 J/m when EMA concentration was increased from 0 to 6 wt %. Beyond 6 wt % of EMA, the increase was marginal. It is quite evident from here that 6 wt % of EMA is just sufficient to compatibilize a 50 : 50 blend of LDPE and PDMS rubber, as this leads to an effective stress dissipation within the polymer matrix. This has been further evidenced from the SEM photomicrograph studies of the blend containing no EMA (Fig. 7) and containing 6 wt % of EMA (Fig. 8).

However, beyond 6 wt % of EMA, it reacts with additional moles of PDMS vinyls present in the system and contributes to marginal improvement in impact strength as well as in adhesion strength properties. The compatibility of polyethylene with PDMS rubber in the presence of the EMA copolymer has been further confirmed by dynamic mechanical analysis studies.

## Dynamic Mechanical Analysis of LDPE–PDMS Rubber Blends Compatibilized with EMA Copolymer

Dynamic mechanical properties such as storage modulus ($E'$), loss modulus ($E''$), and damping (tan $\delta$) of the individual components and that of the blends containing EMA copolymer as a polymeric compatibilizer varying in proportion from 0 to 10 wt % were determined and are depicted in Figures 10–15.

Figure 10 shows the $E'$, $E''$, and tan $\delta$ vs. temperature curves of LDPE after melting and molding at 180°C. The mechanical loss curve (tan $\delta$) shows three distinct relaxations, $\alpha$, $\beta$, and $\gamma$, as observed for branched LDPE containing 15–16 methyl groups for every 1000 carbon atoms.[14] The $\alpha$-transition occurs at +84.7°C, is much below the melting point of LDPE (112°C), and which is believed to be due to molecular motion in the crystalline phase. The $\beta$-transition, which occurs at −17.2°C, is believed to be associated with the onset of motion of the

**Table II Tensile Impact Strength of LDPE–PDMS Rubber Blends Containing EMA**

| Sample Code | Impact Strength (J/m) |
|---|---|
| $PES_0$ | 765 |
| $PES_1$ | 820 |
| $PES_2$ | 980 |
| $PES_4$ | 1570 |
| $PES_6$ | 1720 |
| $PES_{10}$ | 1730 |

Subscripts indicate the proportion of EMA in a 50 : 50 blend of polyethylene and PDMS rubber.

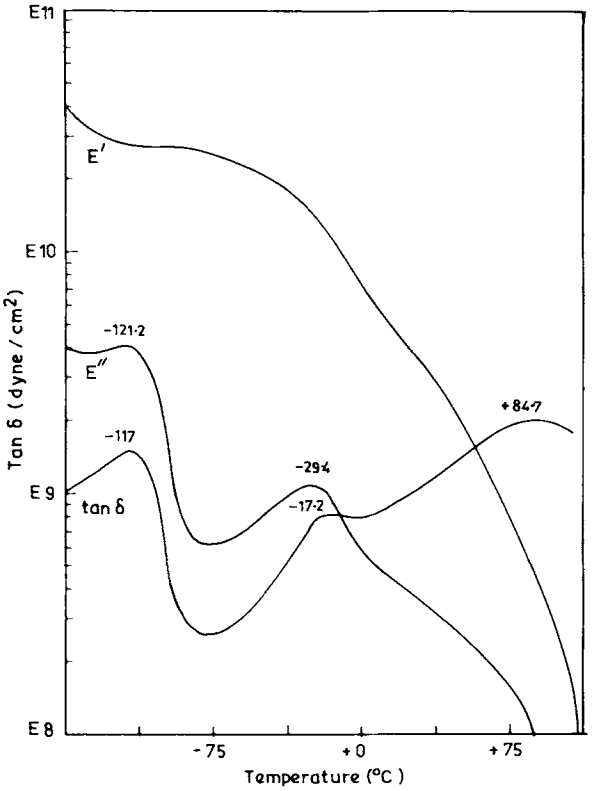


**Figure 10** Temperature dependence of dynamic mechanical properties of pure LDPE.

branch points, i.e., to methyl units. Since the magnitude of this peak is low, therefore the branching in the LDPE is comparatively less, i.e., approximately 15–16 units per 1000 carbon atoms.[14] The $\gamma$-transition occurs at $-117.3$°C, which is primarily believed to be associated with the local, very small, short-range segmental motion of three to four methylene groups in the C—C backbone in the amorphous phase. The temperature corresponding to this transition is primarily associated with the glass transition temperature ($T_g$) of LDPE,[15] because for LDPE containing only a few alkylidens units at the branch points, $T_g$ is always below $-100$°C.[16] For LDPE, being a semicrystalline material, the storage modulus ($E'$) reduces marginally near the $\gamma$-transition temperature region and drastically below $10^8$ near the $\alpha$-transition zone because of appreciable melting of crystallites above room temperature. In such a case, a better estimate of the glass transition is obtained from the maximum loss modulus that occurs just below the $\gamma$-relaxation temperature.[17]

Figure 11 shows the dynamic mechanical properties of PDMS rubber plotted against temperature. The mechanical loss (tan $\delta$) curve shows three relaxations at $-39$, $-68$, and $-117.2$°C, corresponding to the brittle temperature, cold crystallization, and glass transition temperature, respectively. The relaxation in the tan $\delta$ curve at $-39$°C, corresponding to the catastrophic fall in $E'$, is associated with the crystalline melting. The tan $\delta$ peak at $-117.2$°C, where a minor drop in the $E'$ value also was observed, is associated with the $T_g$ of the PDMS. The loss modulus also shows a maximum just below this relaxation zone, i.e., at $-123$°C. A small peak in the tan $\delta$ temperature plot at $-68$°C is believed to be due to cold crystallization.[18]

Figure 12 shows the dynamic mechanical properties of the EMA copolymer plotted against temperature. Similar to that of LDPE, the tan $\delta$–temperature plot shows three distinct relaxations: $\alpha$, $\beta$, and $\gamma$. The $\alpha$-relaxation occurs at +46°C just below the melting temperature of the EMA copolymer (81°C). The storage modulus drops drastically just above room temperature. The $\beta$-transition occurs at $-21.2$°C, which is lower than that of LDPE and is very prominent. This is primarily due to motion at the branch junctions of methylacrylate side groups of the copolymer containing 79% ethylene (i.e., 21% methylacrylate). Simultaneously, a transition occurs at a lower temperature of $-131.2$°C associated with

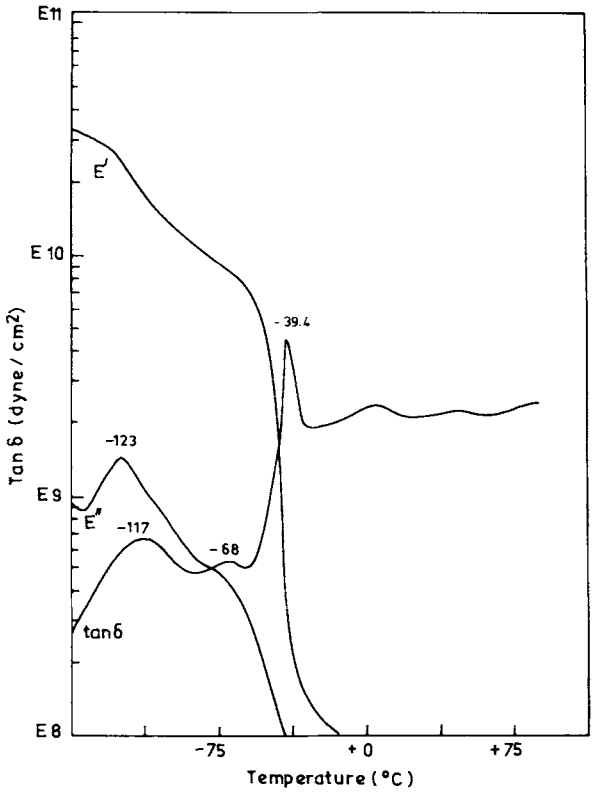


**Figure 11** Temperature dependence of dynamic mechanical properties of pure PDMS rubber.

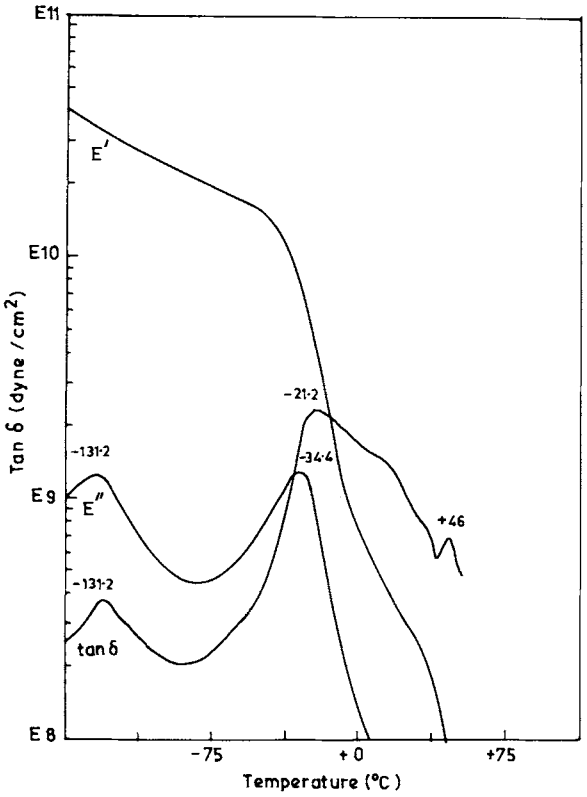


**Figure 12** Temperature dependence of dynamic mechanical properties of EMA copolymer.

a very small, local, short-range and segmental motion of three to four methylene groups in a row and is ascribed to be the familiar $\gamma$-transition temperature of the copolymer.[19] This occurs at a comparatively lower temperature than that of the LDPE due to flexible methylacrylate side groups.

Figure 13 shows the dynamic mechanical properties of the LDPE–PDMS blend in the proportion of 50 : 50. The damping curve exhibits three major relaxations, $\alpha$, $\beta$, and $\gamma$, as usual. The $\alpha$-transition is very broad, occurring from +78 to +83°C, implying the initiation of crystallite melting of LDPE at a lower temperature as compared to that of pure LDPE due to the presence of amorphos PDMS. This is confirmed from the steady decline of the $E'$ from room temperature to 80°C. The $\beta$-transition is lowered by 20°C, which occurs at −37.2°C, near the crystallite melting temperature of PDMS, implying an easier onset of motion at the branch junctions. The $\gamma$-transition is further lowered by 4°C, which occurs at −121.2°C, implying an easier onset of segmental motion of the $-CH_2-$ groups in the amorphous phase and may be assigned as to the plasticizing effect of PDMS rubber in LDPE, which lowers the $\gamma$-relaxation temperature. As expected, the loss modulus maximum occurs at a lower temperature of −122°C.

The dynamic mechanical properties of the terblend with EMA as the third component changes remarkably. Figure 14 shows the $E'$, $E''$, and tan $\delta$ plots of LDPE–PDMS–EMA (50 : 50 : 6) against temperature. The internal friction (tan $\delta$) curve shows three distinct transitions: $\alpha$, $\beta$, and $\gamma$. The $\alpha$-relaxation temperature remains undisturbed with EMA copolymer incorporation in minor proportions of 6 wt %, which occurs at 81°C.

The storage modulus of the terblend decreases in three stages corresponding to the three transition zones. The crystallites start melting at room temperature and it is completed at around 80°C, indicated by a drastic reduction in the $E'$ value from $10^9$ to $10^8$ dynes/cm$^2$.

The $\beta$-transition region is very prominent, occurring at −27.2°C, about 10°C above that observed for the LDPE–PDMS blend, and the magnitude of this peak is very high, indicating a greater restriction on the mobility due to highly branched structures. This is ascribed to the chemical reaction between EMA and PDMS rubber forming EMA-*g*-PDMS rubber.

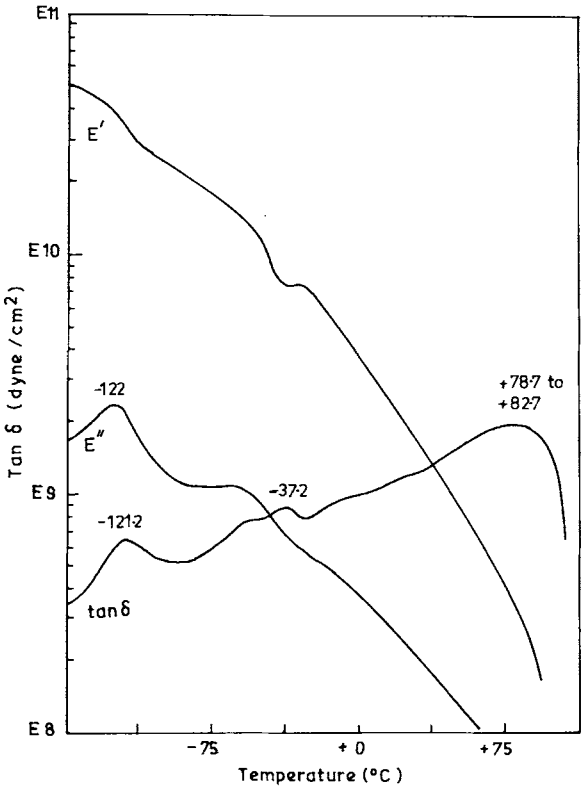


**Figure 13** Temperature dependence of storage modulus, loss modulus, and damping properties of LDPE–PDMS blend in the proportion of 50 : 50.

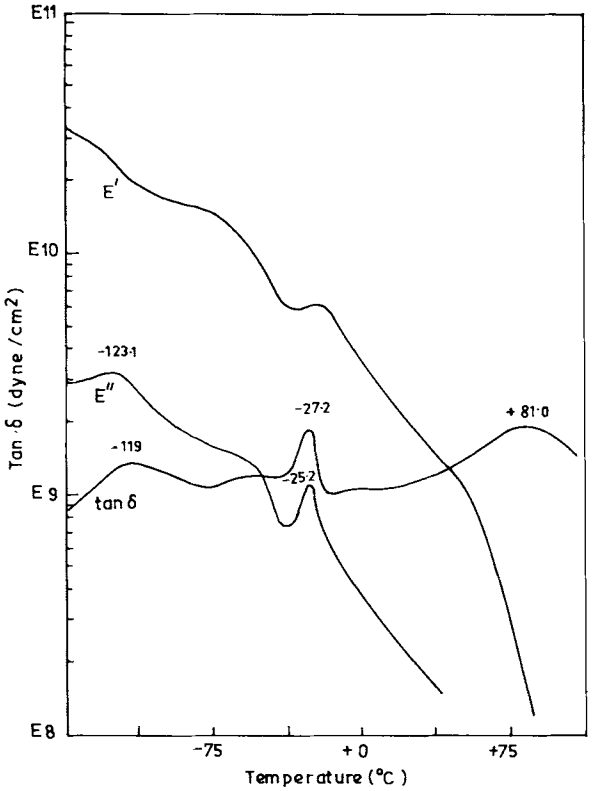


**Figure 14** Temperature dependence of $E'$, $E''$, and tan $\delta$ of LDPE–PDMS–EMA blend in the proportion of 50 : 50 : 6.

The $\gamma$-relaxation peak, corresponding to the $T_g$ of the terblend, is increased by 2°C, occurring at −119°C, as compared to that of binary blend of LDPE–PDMS rubber, indicating a considerable restriction on the segmental mobility of the methylene groups in the amorphous region of the main chain and the cocrystallization of ethylene moieties in EMA-*g*-PDMS with the segmental methylene groups of LDPE in the amorphous phase. This leads to compatibilization of LDPE and PDMS rubber through the *in situ* formation of EMA-*g*-PDMS rubber, which acts as a very good chemical compatibilizer.

Figure 15 shows the dynamic mechanical behavior of the terblend containing 10 wt % of EMA as the third component. The mechanical loss curve shows three distinct relaxation peaks, $\alpha$, $\beta$, and $\gamma$, and a minor relaxation at −93.2°C in between the $\gamma$- and $\beta$-transitions.

The $\alpha$-relaxation peak temperature in the damping curve of the blend remains unaltered at 80.7°C, but it becomes sharper and more distinct compared to the LDPE–PDMS blend, which may be attributed to the formation of larger molecular order in the terblend due to cocrystallization. The storage modulus still shows a three-stage reduction, but not as prominent as in case of the 50 : 50 : 6 terblend. Because of the crystalline melting, the reduction in $E'$ takes place, starting from room temperature to 80°C, where the $\alpha$-transition occurs. The $\beta$-relaxation peak, on the other hand, is very distinct and broad, which appears at −47°C, nearly 10°C lower than that of the LDPE–PDMS rubber blend. This may be due to greater side chain mobility, but the breadth of the relaxation peak indicates the occurrence of more branched structures, leading to a large molecular structure due to more intermolecular bond formation resulting from EMA-*g*-PDMS rubber in the blend.

The $\gamma$-relaxation peak appears as a plateau in the temperature scale from −123.7 to −113.7°C, engulfing the glass transition temperatures of LDPE, PDMS rubber, and LDPE–PDMS rubber blends, indicating good compatibility of the phase components in the presence of 10 pbw of EMA as a reactive compatibilizer. The peak maximum occurs at −118°C, identified as the glass–rubber transition of the compatibilized blend. Broadening of the $\gamma$-relaxation peak is an indication of the presence of mi-

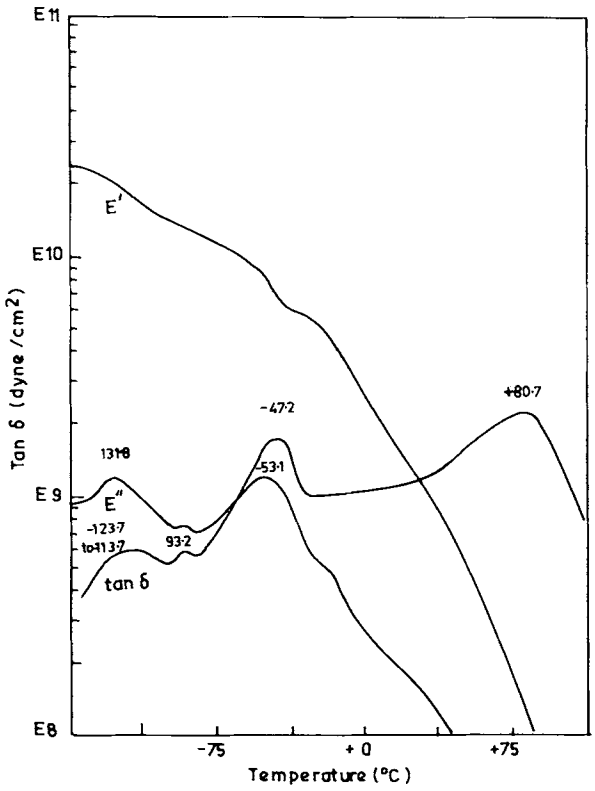


**Figure 15** Temperature dependence of $E'$, $E''$, and tan $\delta$ of LDPE–PDMS–EMA in the proportion of 50 : 50 : 10.

cro inhomogeneity in the system and a tendency toward phase separation.[20]

The appearance of a small peak at −93.2°C, which is higher than the γ-relaxation peak and lower than the β-transition peak, may be explained as due to the rubber–glass transition temperature of EMA-*g*-PDMS rubber formed as a separate phase because of reaction of excess EMA with PDMS rubber at the interface. This disturbs the symmetry within the system beyond 6 wt % of EMA copolymer and reduces crystallinity of the matrix drastically although remaining higher than that observed for the binary blend of LDPE and PDMS rubber. The authors have shown the miscibility of the EMA–PDMS rubber blend in all proportions through a chemical reaction in an earlier communication,[21] which was confirmed by the occurrence of a single composition-dependent glass transition temperature.

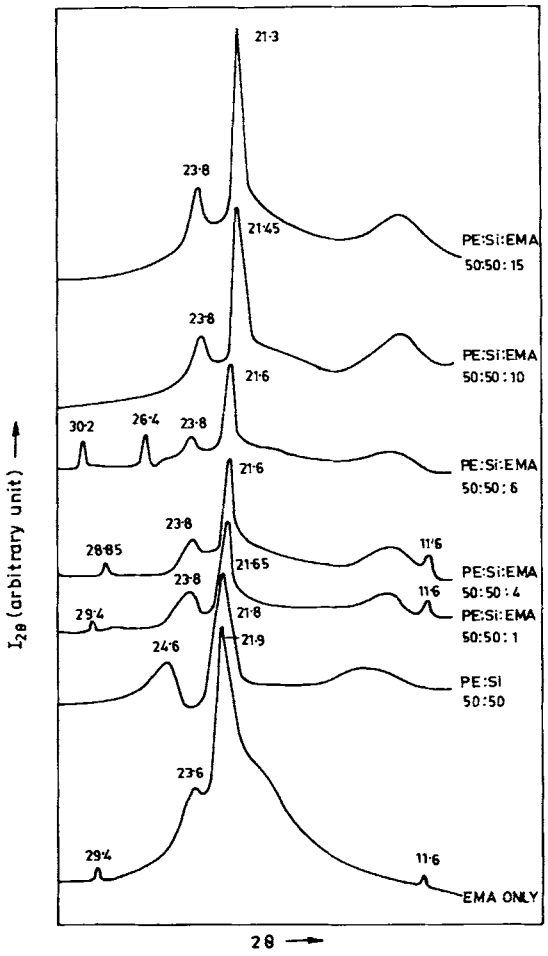


**Figure 16** X-ray diffractograms of EMA, LDPE–PDMS blend, and LDPE–PDMS blend containing various doses of EMA.

## Effect of EMA Copolymer on the Microstructure of the Blends

X-ray diffractograms (XRDS) of neat EMA copolymer, LDPE–PDMS rubber blend, and LDPE–PDMS rubber blend containing various doses of EMA are shown in Figure 16. A broad halo in the region from 7° to 16° 2θ for the LDPE–PDMS rubber blend represents the amorphous part. The sharp peaks at 21.8° and 24.6° 2θ represent the two prominent (1, 1, 0) and (2, 0, 0) reflections of LDPE. The XRD pattern for EMA is partially crystalline with peaks at 11.6, 20.2, 21.9, 23.6, and 29.4° 2θ. On introduction of EMA into the blend of LDPE–PDMS rubber, an initial decrease in the peak intensities of polyethylene (1, 1, 0) and (2, 0, 0) reflections is observed up to 6 wt % of EMA, beyond which it increases. The degree of crystallinity initially increases as compared to the reference blend on the introduction of EMA, which shows an abruptive increase at 6 wt % of EMA, beyond which it decreases again.

There is a gradual shift of the strongest peak toward a lower degree, i.e., from 21.8 to 21.3° 2θ as the EMA concentration increases from 1 to 10 wt % in the 50 : 50 blend of LDPE : PDMS. There is also a shift of the second strongest peak (2, 0, 0) from 24.6° to 23.8° 2θ as EMA is introduced into the system. Besides, it is observed categorically that the sharpness of all the peaks including the size of the halo increases with increase in EMA concentration in the LDPE : PDMS blend. This is conclusive proof for greater ordering in the blends when EMA is added as the third component.

It is quite interesting to note that in the case of the 50 : 50 : 6 blend the peaks at 23.8° and the halo at 16° 2θ reduces its intensity, whereas extra sharp peaks appear at 26.4° and 30.2° 2θ, which were not found in case of the other blends. The peaks that appeared for the blend containing a lower dose of EMA, such as 4 wt %, at 29.4° and 11.6° 2θ disappeared completely. Also, the peak that appeared at 26.4° 2θ has a "*d*" value of 3.37 Å, which does not correspond to any other interplanar spacing of polyethylene. The other peak of 30.2° 2θ corresponds to a (2, 1, 0) reflection of polyethylene that has increased its intensity on blending with EMA. This gives strong evidence for some sort of structural ordering occurring within the blend of LDPE : PDMS containing 6 wt % of EMA, and possibly a new peak thus formed is due to the formation of a totally different structure in the matrix. The peak toward a lower angle of 11.6° 2θ disappears completely. At a higher dosage of EMA, the increase in the intensity of the PDMS halo may be due to some sort of or-

**Table III Degree of Crystallinity (*Xc*), Crystallite Sizes ($P_{110}$, $P_{200}$), Size Anisotropy ($P_{110}/P_{200}$), Paracrystalline Distortion Parameter $\langle g^2 \rangle^{1/2}$, and Interchain Distances (*r*) of the Blends Containing EMA**

| Sample | $P_{110}$ | $P_{200}$ | $\frac{P_{110}}{P_{200}}$ | $\langle g^2_{100} \rangle^{1/2}$ | $\langle g^2_{200} \rangle^{1/2}$ | $r_{110}$ (Å) | *Xc* |
|---|---|---|---|---|---|---|---|
| EMA | 65 | — | — | 0.022 | — | 4.50 | 0.198 |
| $PES_0$ | 148 | 232 | 0.63 | $9.8 \times 10^{-3}$ | $6.0 \times 10^{-3}$ | 4.53 | 0.159 |
| $PES_1$ | 228 | 160 | 1.43 | $6.4 \times 10^{-3}$ | $8.2 \times 10^{-3}$ | 4.56 | 0.159 |
| $PES_4$ | 190 | 133 | 1.43 | $7.6 \times 10^{-3}$ | $9.8 \times 10^{-3}$ | 4.57 | 0.160 |
| $PES_6$ | 205 | 143 | 1.43 | $7.1 \times 10^{-3}$ | $9.2 \times 10^{-3}$ | 4.57 | 0.316 |
| $PES_{10}$ | 148 | 130 | 1.14 | $9.97 \times 10^{-3}$ | 0.010 | 4.59 | 0.194 |

The subscripts of the sample codes represent the proportion of EMA in the blend.

dering brought about in the amorphous region by reaction with EMA.

Table III shows the degree of crystallinity (*Xc*), the crystallite sizes ($P_{110}$, $P_{200}$), the size anisotropy ($P_{110}/P_{200}$), the paracrystalline distortion parameter $\langle g^2 \rangle^{1/2}$, and the interchain distances (*r*) of the blends containing EMA. On introduction of EMA into the blend of LDPE : PDMS, *Xc* increases first, reaches a maximum at 6 wt % of EMA, then decreases. This maxima in *Xc* observed at 6 wt % of EMA for the blend synchronizes with the observed optimum properties of the blend and has been explained as due to the cocrystallization of LDPE with EMA in EMA-*g*-PDMS and this phenomenon is known as isodimorphism.[22]

The crystallite sizes in the (2, 0, 0) direction decreases with increase in EMA concentrations in all three blend proportions, but it increases initially and then decreases for the (110) direction. Size anisotropy for the EMA-containing blends remains more or less constant.

The interchain separation of the blends shows a gradual increase as EMA is introduced into all the blends of LDPE and PDMS rubber studied. Thus, from the X-ray diffraction studies of all the blends, it can be concluded that with 6 wt % of EMA in the blend a recrystallization phenomenon occurs with greater ordering and larger crystalline domains formed in the blend due to cocrystallization or isodimorphism[22] of EMA with polyethylene and reaction of EMA with PDMS rubber. Observation of a new peak at 26.4° $2\theta$ corresponding to a *d*-value of 3.37 Å suggests the formation of a new crystalline phase with a slightly modified structure.

## CONCLUSIONS

The following conclusions may be drawn from the present study:

1. EMA copolymer acts as a good chemical compatibilizer in the blends of LDPE and PDMS rubber.
2. The optimum concentration of EMA required to compatibilize a blend of LDPE : PDMS in a 50 : 50 proportion is found to be 6 wt %.
3. Adhesion between the blend components improves with the incorporation of EMA as the third component.
4. Impact strength improves with EMA content in the blend.
5. The phase morphology changes from a co-continuous to discrete domain in the presence of the optimum concentration of EMA.
6. The degree of crystallinity increases and reaches a maximum at an optimum concentration of EMA copolymer in the blend and new peaks appear due to formation of a modified crystalline structure in the blend.

The authors are thankful to the Council of Scientific and Industrial Research, Government of India, New Delhi, for their financial support in carrying out this work and to Dr. V. K. Tikku of NICCO Corp. for his help and cooperation. The authors also would like to put on record the encouragement received from Mr. A. B. Karnik of Exxon Chemical Eastern Inc., Bombay, during the course of this investigation.

## REFERENCES

1. L. A. Utracki and B. D. Favis, *Polym. Eng. Sci.*, **28**, 1345 (1988).
2. Y. Gallot and C. Wippler, *Makromol. Chem. Macromol. Symp.*, 16 (1988).
3. J. W. Barlow and D. R. Paul, *Polym. Eng. Sci.*, **21**(15), 985 (1981).
4. M. Xanthos, *Polym. Eng. Sci.*, **28**(21), 1392 (1988).
5. G. Serpe, J. Jarrin, and F. Dawans, *Polym. Eng. Sci.*, **30**(9), 553 (1990).

6. R. N. Santra, B. K. Samantaroy, A. K. Bhowmick, V. K. Tikku, and G. B. Nanda, *Plast. Rubber Compos. Process. Appl.*, to appear.
7. J. M. Willis and B. D. Favis, *Polym. Eng. Sci.*, **98**(21), 1416 (1988).
8. A. Molnar and A. Eisenberg, *Polym. Commun.*, **32**(12), 371 (1991).
9. Z. Song and W. E. Baker, *J. Appl. Polym. Sci.*, **44**, 2167–2177 (1992).
10. P. H. Hermans and A. Weidinger, *Makromol. Chem.*, **24**, 44 (1961).
11. D. R. Buchanan, R. L. McCullough, and R. L. Miller, *Acta Crystallogr.*, 20 (1960).
12. L. E. Alexander and E. R. Michalik, *Acta Crystallogr.*, **12**, 105 (1939).
13. I. F. Kovolev, *Opt. Spectrosc.*, **8**, 116 (1990).
14. N. G. McCrum, B. E. Read, and G. Williams, *Anelastic and Dielectric Effects in Polymeric Solids*, Wiley, New York, 1967, p. 366.
15. K. W. Doak, in *Encyclopaedia of Polymer Science and Engineering*, Wiley-Interscience, New York, 1986, Vol. 6, p. 411.
16. N. G. McCrum, B. E. Read, and G. Williams, *Anelastic and Dielectric Effects in Polymeric Solids*, Wiley, New York, 1967, p. 373.
17. N. L. Zutty, J. A. Faucher, and S. Bonotto, in *Encyclopaedia of Polymer Science and Technology*, Interscience, Wiley, Sydney, 1967, Vol. 6, p. 401.
18. J. R. Ebdon, D. J. Hourston, and P. G. Klein, *Polymer*, **25**, 1633 (1984).
19. N. L. Zutty, J. A. Faucher, and S. Bonotto, in *Encyclopaedia of Polymer Science and Technology*, Interscience, Wiley, Sydney, 1967, Vol. 6, p. 296.
20. K. T. Verughese, G. B. Nanda, P. P. De, and S. K. De, *J. Mater. Sci.*, **23**, 3894–3902 (1988).
21. R. N. Santra, S. Roy, A. K. Bhowmick, and G. B. Nando, *Polym. Eng. Sci.*, to appear.
22. T. L. Bluhm, G. K. Hamer, R. H. Marchessault, C. A. Fyre, and P. R. Veregin, *Macromolecules*, **19**, 2861 (1986).

*Received June 18, 1992*
*Accepted November 24, 1992*